

Theoretical Studies of Organometallic Compounds, Part XXXV^[+]

Trends in Molecular Geometries and Bond Strengths of the Homoleptic d¹⁰ Metal Carbonyl Cations [M(CO)_n]^{x+} (M^{x+} = Cu⁺, Ag⁺, Au⁺, Zn²⁺, Cd²⁺, Hg²⁺; n = 1–6): A Theoretical Study**

Anthony J. Lupinetti,^[a] Volker Jonas,^[c] Walter Thiel,^[c] Steven H. Strauss,^{*[b]} and Gernot Frenking^{*[a, b]}

Abstract: Quantum chemical investigations at the MP2 and CCSD(T) level with relativistic effective core potentials for the metals are reported for homoleptic carbonyl complexes of the Group 11 and Group 12 d¹⁰ metal cations with up to six carbonyl ligands. Additional calculations for some compounds were carried out using density functional theory (DFT) methods (BP86 and B3LYP). There is good agreement between theoretical CCSD(T) and experimental bond dissociation energies (BDEs), which are known for eight of the 36 complexes studied. The bond energies predicted by DFT are too high. The complexes [Cu(CO)_n]⁺ and [Au(CO)_n]⁺ are predicted to be bound species for n = 1–5 only, whereas [Ag(CO)_n]⁺ and the Group 12 carbonyls [M(CO)_n]²⁺ are bound species for n = 1–6. The metal–CO bonding has been

analyzed with the help of the natural bond orbital (NBO) method and the charge decomposition analysis (CDA) partitioning scheme. The Group 11 species exhibit more covalent metal–CO bonds than those of Group 12, but coulombic interactions are dominant even for the Group 11 species. The dicarbonyls of Cu⁺, Ag⁺, and Au⁺ have shorter M–CO bonds than the monocarbonyls, and the bond dissociation energies are higher for [M(CO)₂]⁺ than for [M(CO)]⁺. This is explained by the polarization (s–d_σ hybridization) of the metal valence electrons in [M(CO)]⁺. The metal–CO bond energies of the

tricarbonyls are significantly lower than those of the dicarbonyls, because the favorable charge polarization at the metal is not effective. The drop in the bond energy is particularly great for [Au(CO)₃]⁺, because the Au⁺–CO bonds in [Au(CO)]⁺ and [Au(CO)₂]⁺ are enhanced by covalent contributions. [Au(CO)]⁺ and [Au(CO)₂]⁺ have stronger metal–CO bonds than the copper and silver analogues, but the tri- and tetracarbonyls of Au⁺ have weaker bonds than those of Cu⁺ and Ag⁺. The M²⁺–CO bond energies of the Group 12 carbonyls are significantly higher than those of the respective Group 11 carbonyls. Since many of the complexes studied in this paper, particularly those of the Group 12 dications, have not been synthesized yet, the results should prove useful to experimentalists.

Keywords: bonding analysis • bond strength • carbonyl complexes • quantum chemical calculations • transition metals


[a] Prof. Dr. G. Frenking, A. J. Lupinetti
Fachbereich Chemie, Philipps-Universität
Hans-Meerwein-Strasse, D-35037 Marburg (Germany)
Fax: (+49) 6421-28-2189
E-mail: frenking@chemie.uni-marburg.de

[b] Prof. S. H. Strauss, A. J. Lupinetti
Department of Chemistry, Colorado State University
Fort Collins, CO 80523 (USA)
Fax: (+1) 970-491-1801
E-mail: strauss@lamar.colostate.edu

[c] Prof. Dr. W. Thiel, Dr. V. Jonas^[+]
Organisch-Chemisches Institut der Universität
Winterthurerstrasse 190
CH-8057 Zürich (Switzerland)
Fax: (+41) 1-6356836
E-mail: thiel@oci.unizh.ch

[+] Current address:
UCSD/NPACI, San Diego Supercomputer Center, MC 0505,
9500 Gilman Dr., San Diego, CA 92093-0505 (USA)

[+] Part XXXIV: D. V. Deubel, G. Frenking, *J. Am. Chem. Soc.* **1999**, *121*, 2021.

 Supporting information for this article is available on the WWW under <http://www.wiley-vch.de/home/chemistry/> or from the author. Tables S1 and S2 give calculated bond energies and bond lengths of [M(CO)_n]⁺ (M = Cu, Ag, Au; n = 1–4) at different levels of theory. Figure S1 shows the correlation of the calculated bond energies of the same species between CCSD(T)//CCSD(T)/I and CCSD(T)//MP2/I.

Introduction

The chemistry of homoleptic metal carbonyls is an area of intensive research activity.^[1, 2] Cationic complexes $[M(CO)_n]^{x+}$ that were unknown or thought to be too unstable to exist in condensed phases have been isolated as salts of weakly coordinating anions in the last few years.^[1–3] Examples are O_h $[Fe(CO)_6]^{2+}$, D_{4h} $[Pd(CO)_4]^{2+}$, $D_{\infty h}$ and C_{2v} $[Cu(CO)_2]^{+}$, D_{3h} $[Cu(CO)_3]^{+}$, T_d $[Cu(CO)_4]^{+}$, and $D_{\infty h}$ $[Ag(CO)_2]^{+}$, $[Au(CO)_2]^{+}$, $[Hg(CO)_2]^{2+}$.^[1–3] The isolation of $[Ir(CO)_6][Sb_2F_{11}]_3$ demonstrates that even triply charged homoleptic metal carbonyl complexes can be stable with respect to CO dissociation if the counterion is only weakly coordinating.^[2a] It has been suggested that the many cationic homoleptic metal carbonyl complexes that have unusually high $\nu(CO)$ values should be referred to as nonclassical, because their M–CO bonds clearly differ in nature from the M–CO bonds in the majority of metal carbonyls.^[1]

The cationic homoleptic Group 11 carbonyl complexes $[M(CO)_n]^{+}$ ($M = Cu^+$, Ag^+ , Au^+ ; $n \geq 2$) have been the focus of numerous recent experimental studies.^[1–5] Although copper(I) monocarbonyls have been known for a very long time,^[6] evidence for the formation of copper(I) polycarbonyls as discrete, isolable compounds has only recently been reported.^[4, 5a,b] A series of seminal studies by Souma and co-workers demonstrated that Cu^+ ions dissolved in very strong acids such as $BF_3 \cdot H_2O$ or H_2SO_3F can bind up to four CO ligands at certain temperatures and pressures.^[7] Armentrout and co-workers later confirmed the existence of the $[Cu(CO)_4]^{+}$ cation in the gas phase,^[8] and Strauss and co-workers recently determined the structure of a salt containing the T_d $[Cu(CO)_4]^{+}$ complex.^[4] Salts of the $D_{\infty h}$ complexes $[Ag(CO)_2]^{+}$ and $[Au(CO)_2]^{+}$ have been isolated,^[5c,e] and the structure of the silver(I) salt has been reported.^[5c] The pressure of CO required for the solid-state transformation $[M(CO)_2]^{+} \rightarrow [M(CO)_3]^{+}$ varies dramatically from Cu^+ (approximately 1 atm, $[AsF_6]^{-}$ salt)^[5b] to Ag^+ (13 atm, $[Nb(OTeF_3)_6]^{-}$ salt)^[5d] to Au^+ (approximately 100 atm, $[Sb_2F_{11}]^{-}$ salt).^[5f] It is very interesting that such high pressure is needed to form $[Au(CO)_3]^{+}$ in the solid state, since the dicarbonyl complex $[Au(CO)_2]^{+}$ does not lose CO under vacuum whereas both $[Cu(CO)_2]^{+}$ and $[Ag(CO)_2]^{+}$ do. Apparently, $[Au(CO)_3]^{+}$ is the least stable of the three Group 11 tricarbonyl cations with respect to loss of a CO ligand even though $[Au(CO)_2]^{+}$ is the most stable of the three Group 11 dicarbonyl cations, in agreement with Veldkamp and Frenking's previous theoretical study on the silver and gold carbonyls $[M(CO)_n]^{+}$ ($n = 1–3$).^[9]

The only Group 12 carbonyl which has yet been isolated and well characterized is $[Hg(CO)_2]^{2+}$,^[10] although there are reports of Zn^{2+} carbonyl species formed under CO pressure in zinc-substituted zeolites or on the surface of ZnO .^[11] The $D_{\infty h}$ species $[Hg(CO)_2]^{2+}$ has the highest reported average $\nu(CO)$, 2280 cm^{-1} , among the metal carbonyls. Table 1 lists the Group 11 and 12 metal carbonyls for which experimental CO stretching frequencies are known. The increase in the wave-

Table 1. Experimental data for relevant $[M(CO)_n]^{x+}$ complexes.^[a]

Complex	Idealized symmetry ^[b]	$\nu(CO)^{[c]}$ [cm^{-1}]		$R(M-CO)^{[d]}$ [\AA]	$D_o(M-CO)^{[e]}$ [$kcal\ mol^{-1}$]	Refs.
		IR	Raman			
$[Cu(CO)]^{+}$	$C_{\infty v}$	2178			36(2)	5b,8
$[Cu(CO)_2]^{+}$	$D_{\infty h}$	2164	2177		41(1)	5b,8
$[Cu(CO)_2]^{+}$	C_{2v}	2182, 2162		1.901(6)		5f
$[Cu(CO)_3]^{+}$	D_{3h}	2183	2179, 2206		18(1)	5b,8
$[Cu(CO)_4]^{+}$	T_d	2184		1.965(3)	13(1)	5f,8
$[Ag(CO)]^{+}$	$C_{\infty v}$	2208	2206	2.10(1)	21(1)	5c,8
$[Ag(CO)_2]^{+}$	$D_{\infty h}$	2196	2220	2.14(5)	26(1)	5c,8
$[Ag(CO)_3]^{+}$		2191			13(4)	5d,5f,8
$[Ag(CO)_4]^{+}$					11(+4/–1)	5d,5f,8
$[Au(CO)_2]^{+}$	$D_{\infty h}$	2217	2254			5e
$[Au(CO)_3]^{+}$		2212				5f
$[Hg(CO)_2]^{2+}$	$D_{\infty h}$	2278	2281	2.08(1)		10

[a] Only data for salts of highly-fluorinated anions are given. [b] Symmetry determined by X-ray crystallography or by vibrational spectroscopy. [c] From spectra of solid samples; $\nu(CO)$ for gaseous CO is 2143 cm^{-1} . [d] Average metal–carbon bond length; the stated error is the largest esd for the values averaged. [e] Energy of gas-phase dissociation of a single CO ligand from the complex; from ref. [8]; the stated errors are one esd.

numbers upon coordination of CO to a late d-block metal cation has been shown to be due to the effect of the positive charge on the orbitals of CO, which become less polarized towards oxygen. This results in stronger C–O bonding in the cationic complexes than in free CO.^[12, 13] The average $\nu(CO)$ of most transition metal carbonyls is below 2143 cm^{-1} , the value for free CO,^[14] because $M \rightarrow CO$ π backdonation, which is significant for classical metal carbonyls and which involves the transfer of electronic charge from the metal d_{π} orbitals to the degenerate $CO^* \pi$ orbital, leads to a weaker C–O bond. Theoretical analyses of neutral transition metal carbonyls have shown that $M \rightarrow CO$ π backdonation is more important for the overall M–CO bond than $M \leftarrow CO$ σ donation.^[15] Positively charged metal ions should be weaker π donors than the corresponding neutral metal atoms since any given cation M^+ has a higher ionization potential than the neutral atom M. It is therefore understandable that $M \rightarrow CO$ π backdonation in $[M(CO)_n]^{x+}$ complexes may be much less significant than $M \leftarrow CO$ σ donation and that $\nu(CO)$ values of $[M(CO)_n]^{x+}$ complexes may be considerably higher than in related neutral metal carbonyls. A high CO stretching frequency, indicating that the electrostatic effects on the C–O bond are stronger than π backdonation, is the hallmark of a nonclassical metal carbonyl.^[1]

The lack of π backdonation in nonclassical metal carbonyls might be assumed to lead to relatively weak M–CO bonds for these σ -only or σ -mostly species. One might even postulate that the small number of isolable nonclassical metal carbonyls is related to the presumably weak M–CO bonds. However, theoretical calculations have shown clearly that the first bond dissociation energy (BDE) of a CO ligand from $[Ir(CO)_6]^{3+}$ is *higher* than the BDE of $W(CO)_6$.^[16] Hence, M–CO σ donation and the coulombic attraction between the metal cation and CO in nonclassical metal carbonyls can result in very strong M–CO bonds. Therefore the problem with isolating new *cationic* nonclassical metal carbonyls is not intrinsically weak M–CO bonding due to the lack of $M \rightarrow CO$ π backdonation, but the stabilization of the charged species by

one or more weakly coordinating anions. It is likely that many new nonclassical metal carbonyls will be discovered and isolated as newer and less basic weakly coordinating counter-anions come into widespread use.^[3]

It would be very helpful for future experimental studies if M–CO bond energies of proposed metal carbonyl species could be predicted from reliable ab initio calculations. In previous studies we showed that calculated BDEs of transition metal carbonyls at the CCSD(T) level of theory using relativistic effective core potentials are accurate to within ± 3 kcal mol⁻¹ of experimental values.^[17, 18] In this work, we present theoretically predicted equilibrium geometries, sequential M–CO bond energies, and an analysis of the M–CO bonding for 36 Group 11 and Group 12 metal carbonyls $[\text{M}(\text{CO})_n]^{x+}$ ($\text{M}^{x+} = \text{Cu}^+, \text{Ag}^+, \text{Au}^+, \text{Zn}^{2+}, \text{Cd}^{2+}, \text{Hg}^{2+}; n = 1–6$). The information from these results that Zn^{2+} , Cd^{2+} , and more highly coordinated Hg^{2+} carbonyl complexes can be made will be important to experimental chemists. The results are also used to analyze and to understand the bonding in nonclassical metal carbonyl species as well as to show what level of theory is necessary to achieve a good correspondence with experimental gas-phase M–CO bond energies.

Methods

All calculations were carried out with the quasi-relativistic small-core pseudopotentials for the metals developed by the Stuttgart Group.^[19] The basis sets for the valence electrons have at least triple-zeta quality, and have been augmented by an f-type polarization function in some of the calculations.^[20] Standard 6-31G(d)^[21] or TZ2P^[22] basis sets were employed for carbon and oxygen. Some of the basis set combinations I–V (Table 2) have been used in previous studies.^[23]

Table 2. Basis sets used in this study.

Basis	Metal valence basis set	C,O
I ^[a]	(311111/22111/411)	6–31G(d)
II ^[b]	(311111/22111/411/1)	6–31G(d)
III	(311111/22111/411)	TZ2P
IV	(311111/22111/411/1)	TZ2P
V	(311111/22111/3111/1)	TZ2P

[a] ECP1 in reference [23]. [b] ECP2 in reference [23].

The geometries of all the metal carbonyls were optimized at the MP2 level of theory^[24] using basis set I, which is the standard method for geometry optimization in this work. Additional geometry optimizations were carried out for selected compounds at CCSD(T)^[25] and using density functional theory (DFT). The DFT optimizations employed the gradient-corrected functionals BP86^[26] and the three-parameter fit B3LYP.^[27] Sequential M–CO bond energies were calculated at CCSD(T)/I//MP2/I for all the complexes studied. The effect of the different basis sets on the calculated CCSD(T) bond energies was investigated. Bond lengths and bond energies were also determined at BP86/I and B3LYP/I for selected complexes. Vibrational frequencies were calculated at MP2/I. The nature of the M–C and C–O bonds was examined by using the natural bond orbital (NBO)^[28] partitioning scheme, charge decomposition analysis (CDA),^[29] and topological analysis of the electron density distribution.^[30] Unless otherwise noted, the structures discussed in this paper are energy minima. The program packages Gaussian 94,^[31] Molpro,^[32] and ACES II^[33] were employed.

Inspection of the M–CO donor–acceptor interactions was performed by using CDA,^[29] in which the (canonical, natural or Kohn–Sham) molecular

orbitals of the complex are expressed in terms of the MOs of appropriately chosen fragments. In the present case, the natural orbitals (NOs) of the MP2/I wavefunctions of $[\text{M}(\text{CO})_n]^{x+}$ are formed as a linear combination of the orbitals of M^{x+} with a d^{10} electronic configuration as one fragment, and $(\text{CO})_n$ in the geometry of the complex as the second fragment. The orbital contributions are divided into four parts: 1) mixing of the occupied orbitals of $(\text{CO})_n$ and the unoccupied orbitals of M^{x+} (σ donation $\text{M}^{x+} \leftarrow (\text{CO})_n$); 2) mixing of the unoccupied orbitals of $(\text{CO})_n$ and the occupied orbitals of M^{x+} (π backdonation $\text{M}^{x+} \rightarrow (\text{CO})_n$); 3) mixing of the occupied orbitals of both fragments (repulsive polarization $\text{M}^{x+} \leftrightarrow (\text{CO})_n$); and 4) mixing of the vacant orbitals of the two fragments (residual term Δ). The latter term should be approximately zero for true closed-shell interactions. A more detailed presentation is given in reference [29]. For the CDA calculations the program CDA 2.1 was used.^[34] The electron density distribution $\delta(\mathbf{r})$, the gradient vector field $\nabla\varrho(\mathbf{r})$, and the associated Laplacian $\nabla^2\varrho(\mathbf{r})$ were computed using the programs PROAIM, SADDLE, GRID, and GRID-VEC.^[35]

Results and Discussion

Performance of the methods

We have studied carefully the accuracy of the theoretical methods used in this work, to provide guidelines for future investigations in the field. This part of the work was necessarily rather detailed, but we summarize the most important results in this paper. It is important to recognize that without sufficient experience it is not easy to choose the right theoretical level for theoretical calculations of transition metal compounds.

Three experimental parameters can be used to assess the performance of each theoretical level: the C–O stretching frequencies $\nu(\text{CO})$, the M–CO bond distances, and the M–CO bond energies. The experimental $\nu(\text{CO})$ values and M–CO bond lengths in Table 1 are solid-state data for salts of $[\text{M}(\text{CO})_n]^{x+}$ complexes with weakly coordinating anions, whereas our theoretical results are for isolated, gas-phase species. The wavenumbers of the C–O stretching mode and the metal–CO distances in nonclassical metal carbonyl cations can vary significantly for different anions.^[1, 2] However, the experimental M–CO bond dissociation energies for $[\text{Cu}(\text{CO})_n]^+$ and $[\text{Ag}(\text{CO})_n]^+$ ($n = 1–4$) in Table 1 are gas-phase data obtained by Armentrout and co-workers, who measured the bond energies by collision-induced dissociation of CO ligands in a guided ion beam tandem mass spectrometer,^[8] and a comparison with our theoretical results is warranted. The most economical level of theory that gave an excellent correlation with the experimental D_0 values was CCSD(T)/I//MP2/I. From the correlation (Figure 1) it is clear that the calculated bond energies at CCSD(T)/I//MP2/I are very close to the experimental values for the BDEs except for the two most strongly bound species, $[\text{Cu}(\text{CO})]^+$ and $[\text{Cu}(\text{CO})_2]^+$. The theoretically predicted BDEs for $[\text{Cu}(\text{CO})]^+$ ($D_0 = 30.9$ kcal mol⁻¹) and $[\text{Cu}(\text{CO})_2]^+$ ($D_0 = 34.3$ kcal mol⁻¹) are lower than the experimental values (36(2) and 41(1) kcal mol⁻¹).^[8]

To investigate the reason for these differences between theory and experiment, we calculated the Cu⁺–CO bond energies of $[\text{Cu}(\text{CO})_n]^+$ for $n = 1–4$ at CCSD(T) using larger basis sets and different bond lengths predicted at various levels of theory. From the results when basis sets I–V were

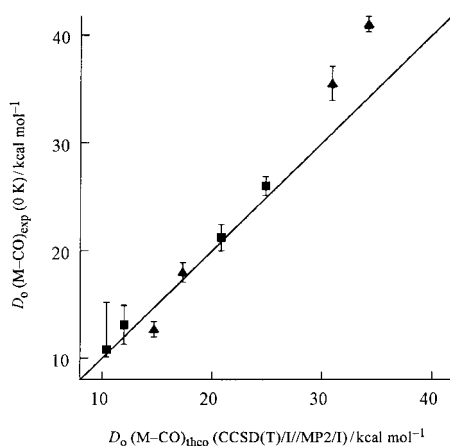


Figure 1. Experimental sequential M–CO bond energies $D_o(\text{M-CO})_{\text{exp}}$ [kcal mol⁻¹] versus theoretical CCSD(T)/I//MP2/I sequential M–CO bond energies $D_o(\text{M-CO})_{\text{theo}}$ [kcal mol⁻¹] for $[\text{Cu}(\text{CO})_n]^+$ (triangles) and $[\text{Ag}(\text{CO})_n]^+$ (squares).

used for the CCSD(T) calculations at geometries obtained at MP2/I, CCSD(T)/I, or CCSD(T)/III (see Table S1 in the Supporting Information) there is hardly any change in the calculated BDEs for the copper carbonyl complexes. At the highest level of theory employed in this study, CCSD(T)/V//CCSD(T)/III using ZPE corrections at MP2/I, the calculated bond energies for $[\text{Cu}(\text{CO})]^+$ ($D_o = 31.2$ kcal mol⁻¹) and $[\text{Cu}(\text{CO})_2]^+$ ($D_o = 34.7$ kcal mol⁻¹) are still 4.3 and 6.3 kcal mol⁻¹ lower than the experimental ones. The reason for the discrepancy is the subject of ongoing work in our group.

The theoretically predicted bond lengths of $[\text{M}(\text{CO})_n]^+$ (M = Cu, Ag, Au; $n = 1-4$) at MP2, CCSD(T), BP86, and B3LYP calculated with different basis sets (see Table S2 in the Supporting Information) demonstrate that MP2/I reproduces faithfully the trend in the M–CO distances predicted at CCSD(T); this is clearly evident in Figure 2, which shows that

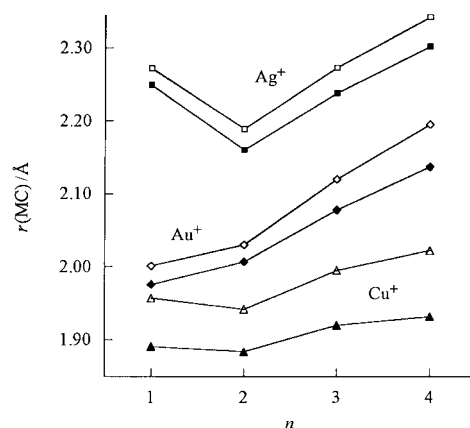


Figure 2. Calculated MP2/I (solid symbols) and CCSD(T)/I (open symbols) M–CO bond lengths of $[\text{M}(\text{CO})_n]^+$ [Å] versus number of carbonyl ligands n .

the bond lengths obtained at MP2/I are all shorter than the corresponding CCSD(T)/I values by nearly the same amount. In particular, the shortening of the M–CO bonds from $[\text{Cu}(\text{CO})]^+$ to $[\text{Cu}(\text{CO})_2]^+$ and from $[\text{Ag}(\text{CO})]^+$ to

$[\text{Ag}(\text{CO})_2]^+$ is predicted correctly. The DFT methods BP86 and B3LYP predict longer Cu–CO bonds in $[\text{Cu}(\text{CO})_2]^+$ than in $[\text{Cu}(\text{CO})]^+$. The good correlation shown in Figure 2 justifies the use of MP2/I-optimized geometries for calculations of bond energies at higher levels of theory. CCSD(T)/I gives very similar BDEs when either MP2/I or CCSD(T)/I-optimized geometry is employed (Table 3). The BDEs

Table 3. Calculated M–CO bond energies (D_o , kcal mol⁻¹) for $[\text{M}(\text{CO})_n]^+$ complexes (M⁺ = Cu, Ag, Au; $n = 1-4$) at five different levels of theory.

	MP2/I// MP2/I	CCSD(T)/I// MP2/I	CCSD(T)/I// CCSD(T)/I	BP86/I// BP86/I	B3LYP/I// B3LYP/I
$[\text{Cu}(\text{CO})]^+$	38.1	32.3	32.9	51.7	43.3
$[\text{Cu}(\text{CO})_2]^+$	43.1	36.2	36.7	47.1	42.6
$[\text{Cu}(\text{CO})_3]^+$	23.4	18.6	19.6	25.0	20.5
$[\text{Cu}(\text{CO})_4]^+$	22.8	16.5	18.0	21.7	17.3
$[\text{Ag}(\text{CO})]^+$	23.3	21.8	22.0	35.2	29.5
$[\text{Ag}(\text{CO})_2]^+$	28.6	26.4	26.6	38.4	33.1
$[\text{Ag}(\text{CO})_3]^+$	13.9	12.6	12.8	16.4	13.8
$[\text{Ag}(\text{CO})_4]^+$	12.3	11.1	11.3	13.0	11.2
$[\text{Au}(\text{CO})]^+$	40.8	38.3	38.5	61.3	49.9
$[\text{Au}(\text{CO})_2]^+$	51	47.0	47.3	57.2	51.9
$[\text{Au}(\text{CO})_3]^+$	9.2	6.4	6.9	11.5	7.2
$[\text{Au}(\text{CO})_4]^+$	9.3	6.7	7.3	10.1	7.1

predicted at MP2/I are only slightly higher than the CCSD(T)/I values, whereas BP86/I and B3LYP/I overestimate the BDEs of the mono- and dicarbonyls. Both DFT methods predict incorrectly that $[\text{Cu}(\text{CO})_2]^+$ has a lower BDE than $[\text{Cu}(\text{CO})]^+$. There is excellent correlation between CCSD(T)/I//CCSD(T)/I and CCSD(T)/I//MP2/I bond energies of $[\text{M}(\text{CO})_n]^+$ (see Figure S1 in Supporting Information). The average difference in D_o is only 0.5 kcal mol⁻¹, and the largest difference is only 1.5 kcal mol⁻¹.

In summary, the results of the calibration study support our use of CCSD(T)/I//MP2/I as the standard level of theory for calculating transition metal carbonyl complexes. Unless otherwise specified, the following discussion is based on the data obtained at this level of theory.

Bond lengths and bond energies

Table 4 shows the calculated bond lengths at MP2/I and the theoretically predicted BDEs D_o and ZPE-corrected D_o values at CCSD(T)/I for all the metal carbonyl complexes investigated. Figure 3 is a graphical representation of the trend in the D_o values. To our knowledge, these are the first published theoretical treatments for any of the six d¹⁰ metal ions for $n > 3$. All 36 combinations examined are predicted to be bound species except for the hexacarbonyls of Cu⁺ and Au⁺. There are four major features (Figure 3): 1) the Group 12 complexes all have larger BDEs than the corresponding Group 11 complexes; 2) the Group 11 complexes show an increase in D_o from $n = 1$ to 2, contrary to the Group 12 complexes; 3) for all complexes, there is a large decrease in D_o from $n = 2$ to $n = 3$; 4) for the heaviest elements Au⁺ and Hg²⁺, the decrease in D_o from $n = 2$ to 3 is much more pronounced than for the other elements. These issues will be discussed in detail below.

Table 4. Predicted M–CO and C–O bond lengths (MP2/I) and M–CO bond energies (CCSD(T)/I//MP2/I). Experimental bond energies are given in parentheses.^[a]

Complex	Symmetry	$r(\text{M}-\text{CO})$ [Å] ^[b]	$r(\text{C}-\text{O})$ [Å] ^[b]	$D_e(\text{M}-\text{CO})$ ^[c] [kcal mol ⁻¹]	$D_o(\text{M}-\text{CO})$ ^[c,d] [kcal mol ⁻¹]
[Cu(CO)] ⁺	$C_{\infty v}$	1.891	1.142	32.3	30.9(36)
[Cu(CO) ₂] ⁺	$D_{\infty h}$	1.884	1.142	36.2	34.3(41)
[Cu(CO) ₃] ⁺	D_{3h}	1.920	1.144	18.6	17.3(18)
[Cu(CO) ₄] ⁺	T_d	1.932	1.146	16.5	14.7(13)
[Cu(CO) ₅] ⁺	C_{3v}	1.928, 1.934, 3.687	1.146, 1.146, 1.148	4.7	4.2
[Cu(CO) ₅] ⁺	D_{3h} ^[e]	1.908, 2.673	1.146, 1.147		
[Cu(CO) ₆] ⁺	O_h ^[e]	2.290	1.148		
[Ag(CO)] ⁺	$C_{\infty v}$	2.249	1.142	21.8	20.8(21)
[Ag(CO) ₂] ⁺	$D_{\infty h}$	2.160	1.142	26.4	24.9(26)
[Ag(CO) ₃] ⁺	D_{3h}	2.238	1.144	12.6	12.0(13)
[Ag(CO) ₄] ⁺	T_d	2.302	1.145	11.1	10.4(11)
[Ag(CO) ₅] ⁺	C_{3v}	2.293, 2.346, 3.641	1.145, 1.145, 1.148	4.9	4.5
[Ag(CO) ₅] ⁺	D_{3h} ^[e]	2.275, 2.851	1.145, 1.147		
[Ag(CO) ₆] ⁺	O_h	2.597	1.147	3.5	3.8
[Au(CO)] ⁺	$C_{\infty v}$	1.976	1.142	38.3	36.9
[Au(CO) ₂] ⁺	$D_{\infty h}$	2.007	1.142	47.0	45.0
[Au(CO) ₃] ⁺	D_{3h}	2.078	1.145	6.4	5.7
[Au(CO) ₄] ⁺	T_d	2.137	1.146	6.7	5.9
[Au(CO) ₅] ⁺	D_{3h}	2.072, 3.124	1.146, 1.148	6.1	6.0
[Au(CO) ₆] ⁺	O_h ^[d]	2.578	1.147		
[Zn(CO)] ²⁺	$C_{\infty v}$	2.017	1.140	74.8	73.3
[Zn(CO) ₂] ²⁺	$D_{\infty h}$	2.011	1.139	65.6	64.0
[Zn(CO) ₃] ²⁺	D_{3h}	2.069	1.141	42.5	41.2
[Zn(CO) ₄] ²⁺	T_d	2.108	1.141	33.6	32.3
[Zn(CO) ₅] ²⁺	D_{3h}	2.136, 2.372	1.142, 1.144	12.8	12.1
[Zn(CO) ₆] ²⁺	O_h	2.299	1.144	14.9	14.1
[Cd(CO)] ²⁺	$C_{\infty v}$	2.255	1.140	55.6	54.4
[Cd(CO) ₂] ²⁺	$D_{\infty h}$	2.228	1.140	52.2	50.7
[Cd(CO) ₃] ²⁺	D_{3h}	2.301	1.141	33.9	32.9
[Cd(CO) ₄] ²⁺	T_d	2.349	1.142	28.9	27.8
[Cd(CO) ₅] ²⁺	D_{3h}	2.398, 2.504	1.143, 1.144	15.7	14.9
[Cd(CO) ₆] ²⁺	O_h	2.500	1.144	16.1	15.3
[Hg(CO)] ²⁺	$C_{\infty v}$	2.164	1.139	70.0	68.7
[Hg(CO) ₂] ²⁺	$D_{\infty h}$	2.126	1.139	67.0	65.2
[Hg(CO) ₃] ²⁺	D_{3h}	2.246	1.141	27.9	27.2
[Hg(CO) ₄] ²⁺	T_d	2.313	1.142	25.3	24.4
[Hg(CO) ₅] ²⁺	D_{3h}	2.318, 2.644	1.142, 1.144	11.2	10.7
[Hg(CO) ₆] ²⁺	O_h	2.530	1.144	10.9	10.5

[a] Reference 8. [b] For five-coordinate complexes, the first value given is for equatorial CO ligands and the other values are for axial CO ligands. [c] Dissociation of a single CO ligand from the complex. [d] ZPE corrections from MP2/I. [e] Not a minimum on the potential energy surface.

All the mono-, di-, tri-, and tetracarbonyl species are energy minima at their $C_{\infty v}$, $D_{\infty h}$, D_{3h} , and T_d conformations, respectively. The recent isolation of a salt of the [Cu(CO)₄]⁺ cation, with a predicted gas-phase first BDE of nearly 15 kcal mol⁻¹, suggests that the Group 12 mono-, di-, tri-, and tetracarbonyls may be isolable species because all 12 complexes have D_o values greater than 20 kcal mol⁻¹. However, isolation of Group 12 [M(CO)_{*n*}]²⁺ complexes will be an experimental challenge: the large positive charge will probably require the weakest possible counterions, since each successive addition of CO to an M²⁺ cation in the solid state is a replacement, not just a ligand addition. Details of the thermodynamic aspects have been discussed elsewhere for [Ag(CO)_{*n*}][B(OTeF₅)₄] ($n=0-2$).^[1c] The salt [Hg(CO)₂][Sb₂F₁₁]₂ has been isolated and characterized by single-crystal X-ray diffraction,^[10] and [Zn(CO)_{*n*}]²⁺ species ($n=1, 2$) have been generated in zeolites and on metal oxide surfaces.^[11]

All the pentacarbonyl species, except [Cu(CO)₅]⁺ and [Ag(CO)₅]⁺, are energy minima in D_{3h} symmetry. For [Au(CO)₅]⁺, the axial Au–CO bonds are 50% longer than the equatorial bond, which indicates that the former bonds are rather weak. The axial and equatorial M–CO bonds of the Group 12 pentacarbonyls differ much less from each other (Table 4). Calculation of the Hessian matrices showed that the D_{3h} forms of [Cu(CO)₅]⁺ and [Ag(CO)₅]⁺ are transition states with one imaginary frequency of A₂ symmetry. Further geometry optimizations led to energy minima with C_{3v} symmetry with one very long axial Cu–CO or Ag–CO distance (Figure 4). The C_{3v} structures of [Cu(CO)₅]⁺ and [Ag(CO)₅]⁺ can be considered to be weakly bonded adducts of the respective tetracarbonyl with an additional CO ligand. The tetracarbonyl moieties with one short M–CO bond in the C_{3v} conformations of [Cu(CO)₅]⁺ and [Ag(CO)₅]⁺ are only slightly distorted from the T_d equilibrium geometries of the respective [M(CO)₄]⁺ complexes (Figure 4, Table 4). Consis-

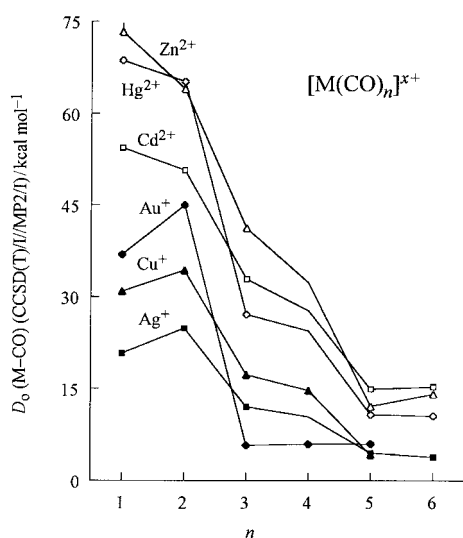


Figure 3. Theoretical sequential M–CO bond energies D_0 [kcal mol⁻¹] versus number of carbonyl ligands n for the 34 bound species in this study: $[M(CO)_n]^+$, solid symbols; $[M(CO)_n]^{2+}$, hollow symbols.

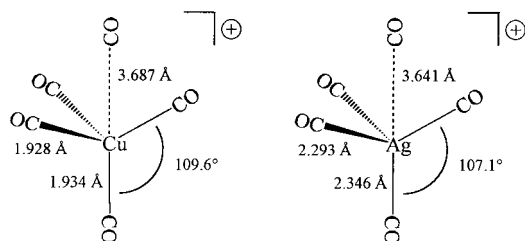


Figure 4. Optimized geometries of $[Cu(CO)_5]^+$ and $[Ag(CO)_5]^+$.

tently with the very long distance between the fifth CO ligand and the Cu^+ or Ag^+ ion, the predicted D_0 values for $[Cu(CO)_5]^+$ and $[Ag(CO)_5]^+$ are both less than 5 kcal mol⁻¹. It is doubtful whether these two species will ever be generated in a condensed phase, unless very low temperatures and very high pressures of CO gas are used.

O_h symmetry was assumed for geometry optimizations of the hexacarbonyls. Calculation of the Hessian matrices at MP2/I showed that the O_h conformations of $[Cu(CO)_6]^+$ and $[Au(CO)_6]^+$ are higher order saddle points on the potential energy surface (each complex had five imaginary frequencies). The octahedral conformations of the other four hexacarbonyl cations, however, are true energy minima on their respective potential energy surfaces. The possibility that very weakly bonded $[Cu(CO)_6]^+$ and $[Au(CO)_6]^+$ species with a symmetry lower than O_h may exist was not pursued.

The D_0 values for the Group 12 carbonyl complexes are significantly higher than those for the corresponding Group 11 complexes—in most cases nearly twice as high. For example, for $[Zn(CO)_2]^{2+}$ and $[Cu(CO)_2]^+$ $D_0 = 64.0$ and 34.3 kcal mol⁻¹, respectively. As discussed below, there is a large electrostatic contribution to the metal–carbon bonds in these complexes, and it is therefore logical that doubly charged Group 12 metal ions attract CO ligands much more strongly than singly charged Group 11 metal ions. The dicarbonyl complexes of the metal ions, except $[Au(CO)_2]^+$, have shorter M–CO bonds than the corresponding monocarbonyl complexes. For each of the Group 11 metal ions, D_0

is higher for the dicarbonyl than for the monocarbonyl complex. Significantly, the opposite is true for the Group 12 complexes. As a general trend, D_0 for $[M(CO)_n]^{x+}$ decreases as n increases from 2 to 6, but there are several interesting exceptions. The sixth CO ligand is more strongly bound than the fifth CO ligand for Zn^{2+} and Cd^{2+} , and D_0 increases slightly from $n = 3$ to $n = 5$ for Au^+ .

The interesting pattern of the Group 11 M–CO bond energies will be discussed below. $[Au(CO)]^+$ and $[Au(CO)_2]^+$ have much higher D_0 values than the Cu^+ or Ag^+ analogues, but $[Au(CO)_3]^+$ and $[Au(CO)_4]^+$ are much more weakly bonded than the Cu^+ and Ag^+ analogues. This is consistent with the experimental observation that $[Au(CO)_3][Sb_2F_{11}]$ is only formed when $[Au(CO)_2][Sb_2F_{11}]$ is treated with more than 100 atm CO whereas $[Cu(CO)_3][AsF_6]$ and $[Ag(CO)_3][Nb(OTeF_5)_6]$ can be synthesized from their respective dicarbonyl precursors at much lower pressure.^[5a,b,d]

Analysis of the bonding situation

What is the nature of the metal–CO bonds in the Group 11 and Group 12 metal carbonyl cations? Can the observed patterns in bond lengths and bond energies be understood in terms of simple chemical principles, derived from an analysis of the calculated data? Information about the bonding interactions between M^+ and M^{2+} and the carbonyl ligands were obtained from the calculated charge distribution and metal-ion valence configurations given by the NBO method^[28] and from the analysis of the electron density distribution^[30] (Tables 5 and 6).

The Group 11 complexes will be considered first. In the $[M(CO)]^+$ monocarbonyls, the metal-ion charge is reduced by only 0.07, 0.05, and 0.15 e relative to the bare metal ions Cu^+ , Ag^+ , and Au^+ , respectively. Since there is very little $M^+ \rightarrow CO$ backdonation (see below), this indicates that the bonding between a single CO ligand and all three M^+ metal ions is largely electrostatic in nature. Nevertheless covalency must also be important, at least for $[Au(CO)]^+$. Purely electrostatic interactions would lead to the incorrect prediction that $[Cu(CO)]^+$ has a greater BDE than $[Au(CO)]^+$, since the metal charge is higher and the M–CO bond is shorter for the copper species. The donation of electron density from the CO ligands to the metal ions is significantly greater in the Group 11 dicarbonyl complexes than in the monocarbonyls: 0.33 e for $[Cu(CO)_2]^+$, 0.27 e for $[Ag(CO)_2]^+$, and 0.46 e for $[Au(CO)_2]^+$. These results are consistent with the D_0 values being larger for the dicarbonyls than for the monocarbonyls. The lower metal-ion charges should result in weaker coulombic contributions to the total bond energy, even after accounting for the shorter M–CO distances in the dicarbonyls. Therefore, the greater D_0 values are the result of significant covalent contributions to the M–CO bonds in all three Group 11 dicarbonyl species. The $OC \rightarrow M^+$ charge donation for the mono- and dicarbonyls calculated by the NBO method shows the same trend as the calculated bond energies (Table 4).

The foregoing conclusion is supported by the calculated energy densities at the bond critical points, H_b (Table 6). It has been shown that the value of H_b is a sensitive probe of the type

Table 5. NBO Results at the MP2/I level. Calculated partial charges at the metal, $q(M)$, total OC \rightarrow metal charge donation Δq ; metal valence orbital population, $d(M)$ and $s(M)$, for the transition metal compounds $[M(CO)_n]^+$ and $[M(CO)_n]^{2+}$.

M	n	$q(M)$	Δq	$d(M)$	$s(M)$
Cu ⁺	1	0.93	0.07	9.77	0.18
	2	0.67	0.33	9.65	0.55
	3	0.75	0.25	9.61	0.49
	4	0.78	0.22	9.55	0.51
	5	0.78	0.22	9.55	0.51
Ag ⁺	1	0.95	0.05	9.91	0.09
	2	0.73	0.27	9.80	0.41
	3	0.75	0.25	9.81	0.36
	4	0.73	0.27	9.82	0.38
	5	0.72	0.28	9.82	0.38
Au ⁺	1	0.85	0.15	9.72	0.38
	2	0.54	0.46	9.57	0.84
	3	0.74	0.26	9.57	0.61
	4	0.81	0.19	9.57	0.52
	5	0.75	0.25	9.56	0.60
Zn ²⁺	1	1.82	0.18	9.91	0.19
	2	1.56	0.44	9.88	0.46
	3	1.49	0.51	9.89	0.51
	4	1.43	0.57	9.89	0.55
	5	1.42	0.58	9.89	0.56
	6	1.37	0.63	9.90	0.60
Cd ²⁺	1	1.86	0.14	9.96	0.14
	2	1.63	0.37	9.93	0.40
	3	1.57	0.43	9.94	0.43
	4	1.50	0.50	9.94	0.49
	5	1.46	0.54	9.94	0.52
	6	1.41	0.59	9.95	0.57
Hg ²⁺	1	1.75	0.25	9.92	0.29
	2	1.42	0.58	9.83	0.71
	3	1.44	0.56	9.88	0.61
	4	1.41	0.59	9.89	0.61
	5	1.37	0.63	9.90	0.63
	6	1.31	0.69	9.93	0.68

of bonding between two atoms: strong covalent bonds have negative values between -1 and -4 Hartree \AA^{-3} and closed-shell interactions (ionic bonds or van der Waals complexes) have $H_b \approx 0$ Hartree \AA^{-3} .^[36] For the $[\text{Cu}(\text{CO})_n]^+$ complexes, the monocarbonyl has a small degree of covalent character (-0.219 Hartree \AA^{-3}), which increases to -0.239 Hartree \AA^{-3} upon formation of the dicarbonyl. The silver complexes follow the same trend, that is, an increase from -0.079 to -0.135 Hartree \AA^{-3} . The gold complexes do not show the same trend, which can be related to the fact that $[\text{Au}(\text{CO})_2]^+$ has a longer bond than $[\text{Au}(\text{CO})]^+$. The Au–C bond in $[\text{Au}(\text{CO})]^+$ has the greatest covalent character among all the Group 11 and Group 12 complexes studied (-0.430 Hartree \AA^{-3+}). The degree of covalency for all silver complexes is lower than for the homologous copper and gold species.

A possible explanation for the peculiar trend from the metal cation monocarbonyls to the dicarbonyls is based on a model suggested previously by Bauschlicher et al., who found a similar trend in the sequential bond energies of $[\text{Cu}(\text{H}_2\text{O})_n]^+$ ($n = 1-4$).^[37] They attributed the rather high bond energy of $[\text{Cu}(\text{H}_2\text{O})_2]^+$ to favorable $4s-3d_{\sigma}$ hybridization, which removes metal-ion electron density from the bonding axis and thereby enhances charge donation from σ -donor ligands along

Table 6. Results of the topological analysis of the wave function calculated at MP2/I for $[\text{M}(\text{CO})_n]^{+2}$ complexes ($n = 1-4$).^[a]

M	n	ρ_b		$\nabla^2\rho_b$		H_b	
		M–C	C–O	M–C	C–O	M–C	C–O
Cu ⁺	1	0.745	3.113	11.299	33.684	-0.219	-5.180
	2	0.761	3.116	11.204	33.325	-0.239	-5.187
	3	0.692	3.098	11.129	32.563	-0.181	-5.149
	4	0.672	3.089	11.005	31.964	-0.167	-5.132
Ag ⁺	1	0.453	3.107	6.167	34.571	-0.079	-5.144
	2	0.557	3.109	7.214	34.296	-0.135	-5.154
	3	0.461	3.097	6.453	33.753	-0.083	-5.123
	4	0.402	3.089	5.650	33.333	-0.060	-5.103
Au ⁺	1	0.943	3.104	8.990	34.236	-0.430	-5.166
	2	0.883	3.110	8.853	33.895	-0.383	-5.177
	3	0.749	3.090	8.421	33.158	-0.275	-5.129
	4	0.658	3.084	7.741	32.864	-0.211	-5.112
Zn ²⁺	1	0.527	3.465	5.416	36.408	-0.126	-5.747
	2	0.610	3.123	7.017	36.838	-0.162	-5.201
	3	0.531	3.118	6.507	35.911	-0.122	-5.189
	4	0.481	3.115	6.067	35.316	-0.100	-5.177
Cd ²⁺	1	0.468	3.116	5.333	37.131	-0.089	-5.179
	2	0.500	3.120	5.572	36.556	-0.110	-5.189
	3	0.416	3.114	5.099	35.765	-0.066	-5.171
	4	0.373	3.110	4.693	35.252	-0.050	-5.160
Hg ²⁺	1	0.645	3.111	5.929	38.520	-0.194	-5.169
	2	0.705	3.121	6.271	37.289	-0.242	-5.197
	3	0.537	3.113	5.836	36.349	-0.130	-5.170
	4	0.464	3.106	5.335	35.626	-0.092	-5.154

[a] Electron density ρ_b ($e \text{\AA}^{-3}$), Laplacian concentration $\nabla^2\rho_b$ ($e \text{\AA}^{-5}$), energy density H_b (Hartree \AA^{-3}) at the bond critical point.

this axis (Figure 5). The same effect can be described as a polarization by a Lewis base of the isotropic charge distribution of the valence shell of a spherical d^{10} metal ion into a disk-shaped valence-electron distribution that lies in the plane

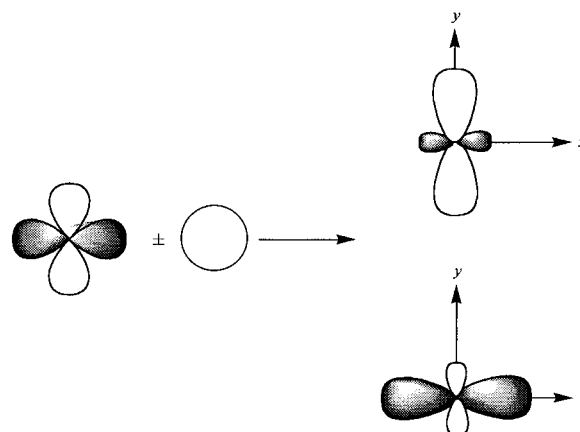


Figure 5. Schematic representation of the $s-d_{\sigma}$ hybridization leading to charge polarization at the d^{10} metal which favors the approach of CO along the x axis.

perpendicular to the bonding axis. This in turn facilitates the approach of a second Lewis base *trans* to the first. Since a majority of the energy cost for the hybridization is paid during the formation of the first M^+ –ligand bond, the second D_o value is higher than the first. Consequently, the large decrease in D_o from $n = 2$ to $n = 3$ can be attributed to the loss of this very favorable $4s-3d_{\sigma}$ hybridization.^[37] Armentrout and co-

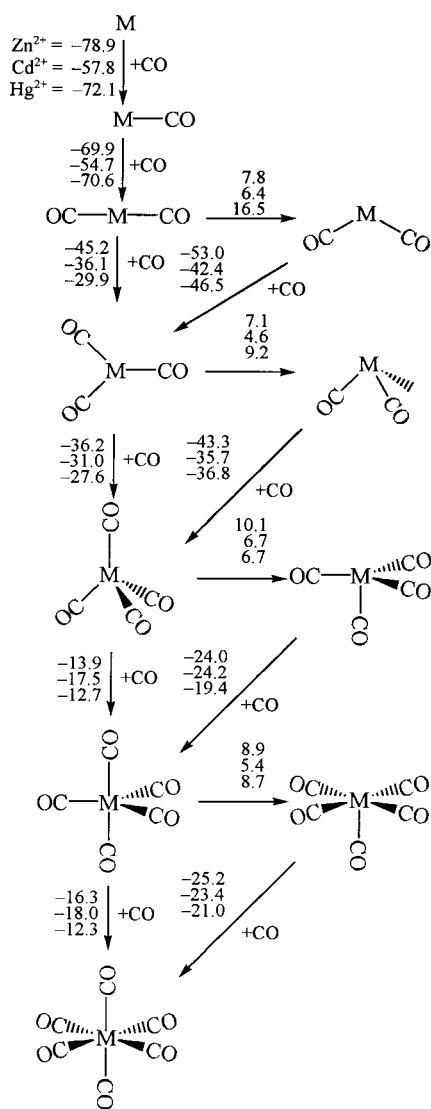


Figure 6. Schematic representation of sequential bond dissociation energies $-D_e$, reorganization energies, and carbonyl bonding energies $-D_e'$ for $[M(CO)_n]^{2+}$. The energies [kcal mol⁻¹] are calculated at the MP2/1//MP2/1 level of theory.

workers explained the bond energy sequences for the series of gas-phase complexes $[Cu(CO)_n]^+$ and $[Ag(CO)_n]^+$ by a similar, albeit qualitative, analysis.^[8] This explanation is essentially the basis for understanding the prevalence of two-coordination in the chemistry of Ag^+ , Au^+ , and Hg^{2+} and has been an enduring paradigm in inorganic chemistry for many years.^[38]

The calculated metal-ion electron populations in Table 5 support the $s-d_\sigma$ hybridization model. The d^{10} valence configurations of the M^+ cations clearly become distorted in the $[M(CO)]^+$ monocarbonyls by $s-d_\sigma$ hybridization: the electronic charges in the metal-ion valence s orbitals are larger than the charge donated to the metal ion by the CO ligand. For example, the CO ligand in $[Au(CO)]^+$ transfers $0.15 e$ to the gold ion, but the Au $6s$ orbital in the complex contains $0.38 e$. The excess metal-ion s orbital charge is equal to the decrease in metal-ion d orbital occupation. The increase in the $OC \rightarrow M^+$ charge donation on going from $[M(CO)]^+$ to $[M(CO)_2]^+$ is clearly greater than the decrease in the metal d

orbital population, confirming that $4s-3d_\sigma$ hybridization makes $M(CO)^+$ a better acceptor (a better Lewis acid) than M^+ . Therefore, it appears that the decrease in electron–electron repulsion between the metal-ion d_σ and CO 5σ orbitals along the bonding axis in $[Au(CO)_2]^+$ more than compensates for the weaker coulombic attraction and the loss of covalency relative to the monocarbonyl complex of Au^+ . The valence s orbital population in $[Au(CO)_2]^+$ is $0.84 e$, whereas it is only $0.55 e$ in $[Cu(CO)_2]^+$ and $0.41 e$ in $[Ag(CO)]^+$.

To understand the particularly large decrease in BDEs from $[Au(CO)_2]^+$ to $[Au(CO)_3]^+$ compared with the other Group 11 di- and tricarbonyls, which is parallel to the decrease from $[Hg(CO)_2]^+$ to $[Hg(CO)_3]^+$ relative to the other Group 12 homologues, we calculated the energy necessary to bend the dicarbonyls from a linear arrangement to $C-M-C = 120^\circ$: for the Group 11 dicarbonyls it is $8.5 \text{ kcal mol}^{-1}$ for $[Cu(CO)_2]^+$, $6.7 \text{ kcal mol}^{-1}$ for $[Ag(CO)_2]^+$, and $21.1 \text{ kcal mol}^{-1}$ for $[Au(CO)_2]^+$; and for the Group 12 carbonyls, $7.8 \text{ kcal mol}^{-1}$ for $[Zn(CO)_2]^{2+}$, $6.4 \text{ kcal mol}^{-1}$ for $[Cd(CO)_2]^{2+}$, and $16.5 \text{ kcal mol}^{-1}$ for $[Hg(CO)_2]^{2+}$. The significantly larger energies which are necessary to bend $[Au(CO)_2]^+$ and $[Hg(CO)_2]^{2+}$ reflect the higher degree of covalency in the linear dicarbonyls of Au^+ and Hg^{2+} . It is the high energy cost of bending the dicarbonyl moieties which yields significantly lower BDEs for $[Au(CO)_3]^+$ and $[Hg(CO)_3]^+$ than for the lighter-element homologues.

An interesting, if not unexpected, phenomenon is revealed by the charge distributions and electronic configurations of the Group 12 metal ions in the complexes in Table 5: the d valence-shell populations are closer to 10 than those of the Group 11 complexes, and the Δq and $s(M)$ values for a given $[M(CO)_n]^{2+}$ complex are virtually the same. This indicates that the CO ligands are donating electron density to the empty metal s orbital with little or no d orbital participation, which suggests that there is hardly any $s-d$ hybridization at the metal in the metal–CO bonds. Only in the case of $[Hg(CO)_2]^{2+}$ is there a clearly larger $s(Hg)$ population than charge donation Δq . Accordingly, the H_b value of $[Hg(CO)_2]^{2+}$ shows an appreciable amount of covalency (Table 6). The differences and trends in the $s-d$ hybridization between Group 11 and Group 12 metal ions can be explained using the $d^9s^1 \leftarrow d^{10}$ promotion energies. The excitation energies are much lower for the Group 11 species Cu^+ (2.72 eV), Ag^+ (4.86 eV), and Au^+ (1.86 eV) than for the Group 12 metal ions Zn^{2+} (9.68 eV), Cd^{2+} (9.97 eV), and Hg^{2+} (5.31 eV).^[39] The heaviest element in each triad has the lowest excitation energy; this is caused by relativistic effects.^[40] Curiously, the D_o values for the Group 12 dicarbonyl complexes are all smaller than for the respective monocarbonyl species, even though the $M-CO$ distances in the dicarbonyls are shorter than in the monocarbonyls. This could be due to the lower positive charge at the metal ions in the dicarbonyl complexes (Table 5), which leads to weaker charge attraction to CO in spite of the shorter bonds.

Two factors determine the pattern of BDEs for the Group 11 and Group 12 metal carbonyl complexes: the degree of covalent bonding in the $M-CO$ bonds, and coulombic interactions. The latter are clearly dominant in the Group 12

carbonyl complexes $[M(\text{CO})_n]^{2+}$, and the trend in BDEs is consistent with the largely ionic character of the bonds. For each of the Group 12 metal ions Zn^{2+} , Cd^{2+} , and Hg^{2+} , the D_0 values are similar for $n = 1$ and 2, for $n = 3$ and 4, and for $n = 5$ and 6 (Figure 3). Figure 6 displays the calculated energies at MP2/I which are necessary to distort the $[M(\text{CO})_n]^{2+}$ species from the equilibrium structure to the geometry in the $[M(\text{CO})_{n+1}]^{2+}$ complexes. It also shows the BDEs of the $[M(\text{CO})_{n+1}]^{2+}$ complexes yielding $[M(\text{CO})_n]^{2+}$ with frozen geometries and with optimized geometries. It is clear that the deformation energies, except for $[\text{Hg}(\text{CO})_2]^{2+}$, are quite similar. Thus, the pattern of BDEs is dominated by the charge attraction between $[M(\text{CO})_n]^{2+}$ in the distorted geometry and CO. This can be explained as follows. The first CO ligand interacts only with M^{2+} . Since the second CO approaches $[M(\text{CO})]^{2+}$ without significant interaction with the first CO and finds only a slightly reduced positive charge at the metal ion, the first two BDEs are very similar. The next CO ligand that approaches the vacant coordination site of the distorted $[M(\text{CO})_2]^{2+}$ or $[M(\text{CO})_3]^{2+}$ experiences steric and electronic repulsions from an array of bound CO ligands at either 120° (two CO ligands) or 109.5° (three CO ligands), respectively. This leads to similar BDEs with respect to the frozen geometries of $[M(\text{CO})_n]^{2+}$, with an intermediate magnitude. The fifth and sixth CO ligands approach the distorted tetra- and pentacarbonyls with bond angles of 90° (four CO ligands in both cases). This leads to BDEs for $[M(\text{CO})_5]^{2+}$ and $[M(\text{CO})_6]^{2+}$ which are very similar and considerably lower than the previous ones. Essentially the same trend in BDEs is found for the Group 11 carbonyl complexes, although the higher covalent contributions yield a slightly different pattern, particularly for the gold complexes (Table 4).

Theoretical studies have shown that the most important factor affecting the covalent bonding in neutral transition metal carbonyls is the $\text{OC} \leftarrow M \pi$ backdonation.^[40] The results of our investigation of the effect of $M^{x+} \rightarrow \text{CO} \pi$ backdonation in the metal carbonyl cations $[M(\text{CO})_n]^{x+}$ ($n = 1-4$) using the CDA method^[29] are listed in Table 7. The CDA partitioning scheme results in absolute values for the $\text{OC} \rightarrow M^{x+}$ donation and $M^{x+} \rightarrow \text{CO}$ backdonation that are less meaningful than the ratio of the two values, backdonation/donation (b/d), which expresses the relative amounts of the two contributions to the covalent bonding; therefore b/d will be discussed.

The following conclusions can be drawn from the CDA data. There is only negligible $M^{2+} \rightarrow \text{CO} \pi$ backdonation in the Group 12 metal-ion carbonyls. This is in agreement with the NBO results and the topological analysis of the density distributions, which indicate only weak covalent interactions in $M^{2+} - \text{CO}$ bonds caused by charge donation from CO to the metal valence s orbitals. Distinct $M^+ \rightarrow \text{CO}$ backdonation is found in the Group 11 carbonyl cations. The b/d ratio clearly increases in the order $\text{Ag}^+ < \text{Cu}^+ < \text{Au}^+$ for all four values of n . The backdonation is particularly large for $[\text{Au}(\text{CO})]^{2+}$ and $[\text{Au}(\text{CO})_2]^{2+}$. This is caused by relativistic effects, which are manifested in two ways:^[40] 1) by the shrinkage of s orbitals and the expansion of d orbitals, which allow for more effective $\text{Au}^+ \rightarrow \text{CO} \pi$ backdonation; 2) by the very low $d^9s^1 \leftarrow d^{10}$ promotion energy of Au^+ . Moreover, the b/d ratio of $[M(\text{CO})_n]^{2+}$ shows the same trend for a given M^+ and n as

Table 7. MP2/I charge decomposition analysis (Per CO) of the metal–ligand interaction for $[M(\text{CO})_n]^{x+}$ ($M = \text{Cu}, \text{Ag}, \text{Au}; n = 1-4$) and $[M(\text{CO})_n]^{2+}$ ($M = \text{Zn}, \text{Cd}, \text{Hg}; n = 1-4$) where M^{x+} is the acceptor and $[(\text{CO})_n]$ is the donor.

M	<i>n</i>	Backdonation ($M \rightarrow \text{CO}$)	Donation ($\text{OC} \rightarrow M$)	Repulsion ($M \rightarrow \text{CO}$)	Residual Δ	<i>b/d</i>
Cu^+	1	0.060	0.537	−0.047	−0.018	0.112
	2	0.058	0.463	−0.022	−0.022	0.125
	3	0.058	0.528	−0.039	−0.016	0.110
	4	0.056	0.549	−0.037	−0.029	0.103
Ag^+	1	0.013	0.327	−0.080	0.002	0.040
	2	0.025	0.359	−0.065	−0.080	0.070
	3	0.020	0.328	−0.079	−0.002	0.061
	4	0.016	0.326	−0.071	−0.001	0.049
Au^+	1	0.109	0.425	−0.131	0.024	0.256
	2	0.084	0.356	−0.066	−0.009	0.236
	3	0.067	0.362	−0.138	0.014	0.185
	4	0.056	0.392	−0.122	0.012	0.142
Zn^{2+}	1	0.001	0.561	−0.021	−0.014	0.002
	2	0.003	0.581	−0.021	−0.017	0.004
	3	0.002	0.522	−0.027	−0.007	0.004
	4	0.001	0.478	−0.027	−0.008	0.002
Cd^{2+}	1	−0.003	0.405	−0.047	0.013	−0.007
	2	−0.001	0.376	−0.041	0.000	0.003
	3	0.001	0.382	−0.042	0.005	0.002
	4	0.001	0.369	−0.039	0.001	0.002
Hg^{2+}	1	0.006	0.459	−0.070	0.013	0.013
	2	0.012	0.403	−0.051	−0.005	0.030
	3	0.006	0.428	−0.068	0.005	0.014
	4	0.004	0.409	−0.064	0.001	0.010

the H_b values in Table 6. It follows that the $M^+ \rightarrow \text{CO}$ backdonation is very important for the covalent character of the bond. Conventional wisdom is that an increase in π backbonding leads to a stronger $M - \text{CO}$ bond in metal carbonyls; for example, experimental $M - \text{CO}$ BDEs increase from $[\text{Cu}(\text{CO})_n]^{2+}$ to $[\text{Ni}(\text{CO})_n]$ to $[\text{Co}(\text{CO})_n]^{2+}$,^[8, 41] and most chemists would attribute this to an increase in π backbonding. The present results suggest that a decrease in π backbonding does *not* always yield weaker bonds. From the calculated BDEs in Table 4, the complexes with the least π backbonding, $[\text{Zn}(\text{CO})_n]^{2+}$, are predicted to have, in general, the strongest $M - \text{CO}$ bonds among the metal ion carbonyl complexes. The same result has been found for the BDEs of the isoelectronic hexacarbonyls $[M(\text{CO})_6]^q$ ($M = \text{Hf}^{2-}, \text{Ta}^-, \text{W}, \text{Re}^+, \text{Os}^{2+}, \text{Ir}^{3+}$).^[16]

That a $[\text{Cu}(\text{CO})_n]^{2+}$ complex has a higher D_0 than the corresponding $[\text{Ag}(\text{CO})_n]^{2+}$ species is due partly to less covalent bonding and partly to the difference in the ionic radii of Cu^+ (0.96 Å) and Ag^+ (1.26 Å).^[42] The longer $\text{Ag}^+ - \text{CO}$ distances also lead to weaker coulombic interactions. The covalent radius of gold is smaller than that of silver^[43] (estimated values: $\text{Ag}, 1.33 \text{ \AA}; \text{Au}, 1.25 \text{ \AA}$).^[43a] Strong covalent contributions result in stronger $M - \text{CO}$ BDEs for the gold carbonyls with $n = 1, 2$. The $\text{Au}^+ \leftrightarrow \text{CO}$ repulsion for $n = 3, 4$ (Table 7) is larger than for any of the Cu^+ and Ag^+ species, and this also explains the weak bonding of $[\text{Au}(\text{CO})_n]^{2+}$ for $n = 3-5$. The surprising stability of $[\text{Ag}(\text{CO})_6]^{2+}$ may be due to the balance between the $\text{Ag}^+ - \text{CO}$ coulombic attraction and the repulsion among the carbonyl ligands, which appear to be more favorable than those in the copper and gold hexacarbonyls.

Conclusion

The results of this study can be summarized as follows.

1. All $[M(\text{CO})_n]^{2+}$ ($M = \text{Zn}, \text{Cd}, \text{Hg}; n = 1-6$) Group 12 metal-ion carbonyls are energy minima in their highest possible symmetric forms. The Group 11 complexes $[\text{Cu}(\text{CO})_n]^+$ and $[\text{Au}(\text{CO})_n]^+$ are predicted to be bound species for $n = 1-5$ only, whereas the $[\text{Ag}(\text{CO})_n]^+$ species are energy minima for $n = 1-6$.
2. In the Group 12 species $[M(\text{CO})_n]^{2+}$, the bond strengths show the trend $M = \text{Zn}^{2+} > \text{Hg}^{2+} > \text{Cd}^{2+}$. For each metal, the strength of the $M-\text{CO}$ bonds is similar for $n = 1, 2$, medium for $n = 3, 4$, and rather weak for $n = 5, 6$.
3. For a given n , the Group 11 cations $[M(\text{CO})_n]^+$ all have weaker $M-\text{CO}$ bonds than the corresponding Group 12 dications. The dicarbonyls have higher BDEs than the monocarbonyls $[M(\text{CO})]^+$. For $n = 1, 2$, the trend in the bond strengths is $M = \text{Au}^+ > \text{Cu}^+ > \text{Ag}^+$, whereas Au^+ has the weakest bonds for $n = 3, 4$.
4. The bonding pattern of the metal ion carbonyls can be explained by the nature of the $M^{x+}-\text{CO}$ bonding interactions. The Group 12 carbonyls $[M(\text{CO})_n]^{2+}$ exhibit mainly coulombic $M^{x+}-\text{CO}$ interactions. Covalent contributions are in general quite small, except for $[\text{Hg}(\text{CO})]^{2+}$ and $[\text{Hg}(\text{CO})_2]^{2+}$. Covalent contributions become significant for the $M^+-\text{CO}$ bonds of Group 11 metal carbonyls $[M(\text{CO})_n]^+$, particularly for $[\text{Au}(\text{CO})]^+$ and $[\text{Au}(\text{CO})_2]^+$. The $s-d_\sigma$ hybridization at the metal ions is the reason for the stronger BDEs exhibited by the dicarbonyls $[M(\text{CO})_2]^+$ than by the monocarbonyls $[M(\text{CO})]^+$. The analysis of the $M^{x+}-\text{CO}$ interactions shows that there is little $M^{x+} \rightarrow \text{CO}$ backdonation.
5. The theoretically predicted bond energies at CCSD(T)/I//MP2/I are in good agreement with experimental results. BP86/I and B3LYP/I give bond energies which are too high. Both DFT methods have problems when applied to the monocarbonyls.

Note added in proof: After our manuscript was submitted we were informed about a recent high-level theoretical study of $[\text{Au}(\text{CO})]^+$ at the CCSD(T) level with very large basis sets which gives without BSSE correction a bond energy $D_e = 48.4 \text{ kcal mol}^{-1}$ (T. K. Dargel, R. H. Hertwig, W. Koch, H. Horn, *J. Chem. Phys.* **1988**, *108*, 3876), which is higher than our value. We are currently investigating the bond energies of the mono- and dicarbonyls of the Group 11 and 12 metal ions at similarly high levels of theory. Preliminary calculations show that the trend of the bond energies does not change with higher quality calculations.

Acknowledgment

This work was supported by the Deutsche Forschungsgemeinschaft (SFB 260 and Graduiertenkolleg Metallorganische Chemie), the Fonds der Chemischen Industrie, the Schweizerischer Nationalfonds, and the U.S. National Science Foundation (CHE-9628769). Computer time was provided by the Hochschulrechenzentrum of the Philipps-Universität Marburg, the HLRZ Darmstadt, the HLRZ Stuttgart, the Swiss Center for Scientific Computing (SCSC Manno), and the C4 Cluster at the ETH Zürich.

- [1] a) A. J. Lupinetti, G. Frenking, S. H. Strauss, *Prog. Inorg. Chem.* submitted; b) A. J. Lupinetti, G. Frenking, S. H. Strauss, *Angew. Chem.* **1998**, *110*, 2229; *Angew. Chem. Int. Ed. Engl.* **1998**, *37*, 2113.

- [2] a) H. Willner, F. Aubke, *Angew. Chem.* **1997**, *109*, 2506; *Angew. Chem. Int. Ed. Engl.* **1997**, *36*, 2402; b) S. H. Strauss, *Chemtracts—Inorg. Chem.* **1997**, *10*, 77; c) F. Aubke, C. Wang, *Coord. Chem. Rev.* **1994**, *137*, 483.
- [3] a) C. A. Reed, *Acc. Chem. Res.* **1998**, *31*, 133; b) A. J. Lupinetti, S. H. Strauss, *Chemtracts—Inorg. Chem.* **1998**, *11*, 565; c) K. Seppelt, *Angew. Chem.* **1993**, *105*, 1074; *Angew. Chem. Int. Ed. Engl.* **1993**, *32*, 1025; d) S. H. Strauss, *Chem. Rev.* **1993**, *93*, 927; e) M. Bochmann, *Angew. Chem.* **1992**, *104*, 1206; *Angew. Chem. Int. Ed. Engl.* **1992**, *31*, 1181.
- [4] a) S. V. Ivanov, S. M. Miller, O. P. Anderson, K. A. Solntsev, S. H. Strauss, unpublished results; b) O. G. Polyakov, S. M. Miller, O. P. Anderson, S. H. Strauss, unpublished results.
- [5] a) J. J. Rack, S. H. Strauss, *Catal. Today* **1997**, *36*, 99; b) J. J. Rack, J. D. Webb, S. H. Strauss, *Inorg. Chem.* **1996**, *35*, 277; c) P. K. Hurlburt, J. J. Rack, J. S. Luck, S. F. Dec, J. D. Webb, O. P. Anderson, S. H. Strauss, *J. Am. Chem. Soc.* **1994**, *116*, 10003; d) J. J. Rack, B. Moasser, J. D. Gargulak, W. L. Gladfelder, H. D. Hochheimer, S. H. Strauss, *J. Chem. Soc. Chem. Commun.* **1994**, 685; e) H. Willner, J. Schaebs, G. Hwang, F. Mistry, R. Jones, J. Trotter, F. Aubke, *J. Am. Chem. Soc.* **1992**, *114*, 8972; f) S. H. Strauss et al., unpublished results.
- [6] a) K. D. Karlin, Z. Tyecklár, A. Farooq, M. S. Haka, P. Ghosh, R. W. Cruse, Y. Gultneh, J. C. Hayes, P. J. Toscano, J. Zubieta, *Inorg. Chem.* **1992**, *32*, 1436; b) M. Pasquali, C. Floriani, in *Copper Coordination Chemistry: Biochemical and Inorganic Perspectives* (Eds.: K. D. Karlin, J. Zubieta), Adenine Press, Guilderland (NY), **1983**, p. 311; c) I. J. Bruce, *J. Organomet. Chem.* **1972**, *44*, 209; d) O. H. Wagner, *Z. Anorg. Chem.* **1931**, *196*, 364; e) Berthelot, *Ann. Chim. Phys.* **1856**, *346*, 477; f) F. Leblanc, *C.R. Acad. Sci. Paris* **1850**, *30*, 483.
- [7] a) Y. Souma, H. Kawasaki, *Catal. Today* **1997**, *36*, 91; b) Y. Souma, H. Sano, *Chem. Lett.* **1973**, 1059; c) Y. Souma, J. Iyoda, H. Sano, *Inorg. Chem.* **1976**, *15*, 968.
- [8] F. Meyer, Y. M. Chen, P. Armentrout, *J. Am. Chem. Soc.* **1995**, *117*, 4071.
- [9] A. Veldkamp, G. Frenking, *Organometallics* **1993**, *12*, 4613.
- [10] a) M. Bodenbinder, G. Balzer-Jöllenbeck, H. Willner, R. J. Batchelor, F. W. B. Einstein, C. Wang, F. Aubke, *Inorg. Chem.* **1996**, *35*, 82; b) H. Willner, M. Bodenbinder, C. Wang, F. Aubke, *J. Chem. Soc. Chem. Commun.* **1994**, 1189.
- [11] a) J. Lin, P. Jones, J. Guckert, E. I. Solomon, *J. Am. Chem. Soc.* **1991**, *113*, 8312; b) G. Hussain, N. Sheppard, *Spectrochim. Acta* **1987**, *43A*, 1631; c) G. Ghiotti, F. Boccuzzi, R. Scala, *J. Catal.* **1985**, *92*, 79; d) Y. Y. Huang, *J. Catal.* **1980**, *61*, 461.
- [12] a) A. S. Goldman, K. Krogh-Jespersen, *J. Am. Chem. Soc.* **1996**, *118*, 12159; b) A. Lupinetti, S. Fau, G. Frenking, S. H. Strauss, *J. Phys. Chem. A.* **1997**, *101*, 9551.
- [13] V. Jonas, W. Thiel, *Organometallics* **1998**, *17*, 353.
- [14] K. P. Huber, G. Herzberg, *Constants of Diatomic Molecules*; Van Nostrand—Reinhold, New York, **1979**.
- [15] E. R. Davidson, K. L. Kunze, F. B. C. Machado, S. J. Chakravorty, *Acc. Chem. Res.* **1993**, *26*, 628, and references therein.
- [16] R. K. Szilagy, G. Frenking, *Organometallics* **1997**, *16*, 4807.
- [17] a) A. W. Ehlers, S. Dapprich, S. F. Vyboishchikov, G. Frenking, *Organometallics* **1996**, *15*, 105; b) A. W. Ehlers, G. Frenking, *Organometallics* **1995**, *14*, 423; c) A. W. Ehlers, G. Frenking, *J. Am. Chem. Soc.* **1994**, *116*, 1514.
- [18] G. Frenking, I. Antes, M. Böhme, S. Dapprich, A. W. Ehlers, V. Jonas, A. Neuhaus, M. Otto, R. Stegmann, A. Veldkamp, S. F. Vyboishchikov, in *Reviews in Computational Chemistry*, Vol. 8 (Eds.: K. B. Lipkowitz, D. B. Boyd), VCH, New York, **1996**, pp. 63–144.
- [19] a) M. Dolg, U. Wedig, H. Stoll, H. Preuss, *J. Chem. Phys.* **1987**, *86*, 866; b) D. Andrae, U. Häussermann, M. Dolg, H. Stoll, H. Preuss, *Theor. Chim. Acta* **1990**, *77*, 123.
- [20] A. W. Ehlers, M. Böhme, S. Dapprich, A. Gobbi, A. Höllwarth, V. Jonas, K. F. Köhler, R. Stegmann, A. Veldkamp, G. Frenking, *Chem. Phys. Lett.* **1993**, *208*, 111.
- [21] W. J. Hehre, R. Ditchfield, J. A. Pople, *J. Chem. Phys.* **1972**, *56*, 2257.
- [22] a) T. H. Dunning, Jr. *J. Chem. Phys.* **1971**, *55*, 716; b) T. H. Dunning, Jr. *J. Chem. Phys.* **1989**, *90*, 1007.
- [23] a) V. Jonas, W. Thiel, *J. Chem. Phys.* **1996**, *105*, 3636; b) V. Jonas, W. Thiel, *J. Chem. Phys.* **1995**, *102*, 8474.

- [24] a) C. Møller, M. S. Plesset, *Phys. Rev.* **1934**, *46*, 618; b) J. S. Binkley, J. A. Pople, *Int. J. Quantum Chem.* **1975**, *9*, 229.
- [25] a) J. Cizek, *J. Chem. Phys.* **1966**, *45*, 4256; b) J. Cizek, *Adv. Chem. Phys.* **1966**, *14*, 35; c) J. A. Pople, R. Krishnan, H. B. Schlegel, J. S. Binkley, *Int. J. Quantum Chem.* **1978**, *14*, 545; d) R. J. Bartlett, G. D. Purvis, *Int. J. Quantum Chem.* **1978**, *14*, 561; e) G. D. Purvis, R. J. Bartlett, *J. Chem. Phys.* **1982**, *76*, 1910; f) J. Noga, R. J. Bartlett, *J. Chem. Phys.* **1987**, *86*, 7041; g) K. Raghavachari, G. W. Trucks, J. A. Pople, M. Head-Gordon, *Chem. Phys. Lett.* **1989**, *157*, 479.
- [26] a) A. D. Becke, *Phys. Rev. A* **1988**, *38*, 3098; b) J. P. Perdew, *Phys. Rev. B* **1986**, *33*, 8822; **1986**, *34*, 7406.
- [27] a) A. D. Becke, *J. Chem. Phys.* **1993**, *98*, 5648; b) P. J. Stevens, F. J. Devlin, C. F. Chabrowski, M. J. Frisch, *J. Phys. Chem.* **1994**, *98*, 11623.
- [28] A. E. Reed, L. A. Curtiss, F. Weinhold, *Chem. Rev.* **1988**, *88*, 899.
- [29] S. Dapprich, G. Frenking, *J. Phys. Chem.* **1995**, *99*, 9352.
- [30] R. F. W. Bader, *Atoms in Molecules. A Quantum Theory*, Oxford University Press, Oxford, **1990**.
- [31] Gaussian 94, M. J. Frisch, G. W. Trucks, H. B. Schlegel, P. M. W. Gill, B. G. Johnson, M. A. Robb, J. R. Cheeseman, T. A. Keith, G. A. Petersson, J. A. Montgomery, K. Raghavachari, M. A. Al-Laham, V. G. Zakrzewski, J. V. Ortiz, J. B. Foresman, J. Cioslowski, B. B. Stefanov, A. Nanayakkara, M. Challacombe, C. Y. Peng, P. Y. Ayala, W. Chen, M. W. Wong, J. L. Andres, E. S. Replogle, R. Gomberts, R. L. Martin, D. J. Fox, J. S. Binkley, D. J. Defrees, I. Baker, J. J. P. Stewart, M. Head-Gordon, C. Gonzalez, J. A. Pople, Gaussian Inc., Pittsburgh (PA), **1995**.
- [32] MOLPRO is a package of ab initio programs written by H.-J. Werner and P. J. Knowles, with contributions from J. Almlöf, R. D. Amos, M. J. O. Deegan, S. T. Elbert, C. Hampel, W. Meyer, K. A. Peterson, R. M. Pitzer, A. J. Stone, and P. R. Taylor.
- [33] ACES II is a package of ab initio programs written by J. F. Stanton, J. Gauss, J. D. Watts, W. J. Lauderdale, and R. J. Bartlett.
- [34] CDA 2.1 is a program written by S. Dapprich and G. Frenking. It is available from anonymous ftp server: ftp.chemie.uni-marburg.de (/pub/cda).
- [35] F. W. Biegler-König, R. F. W. Bader, T. Ting-Hua, *J. Comput. Chem.* **1982**, *3*, 317.
- [36] D. Cremer, E. Kraka, *Angew. Chem.* **1984**, *96*, 612; *Angew. Chem. Int. Ed. Engl.* **1984**, *23*, 627.
- [37] C. W. Bauschlicher, Jr., S. R. Langhoff, H. Partridge, *J. Chem. Phys.* **1991**, *94*, 2068.
- [38] a) J. D. Dunitz, L. E. Orgel, *Adv. Inorg. Chem. Radiochem.* **1960**, *2*, 1; b) C. S. G. Phillips, R. J. P. Williams, *Inorganic Chemistry, Part II*, Oxford University Press, Oxford, **1966**, p. 484.
- [39] C. E. Moore, *Natl. Bur. Stand. Circ. 467*, U.S. GPO, Washington, D.C., **1952**.
- [40] P. Pyykkö, *Chem. Rev.* **1988**, *88*, 563.
- [41] L. S. Sunderlin, D. Wang, R. R. Squires, *J. Am. Chem. Soc.* **1993**, *115*, 12060.
- [42] E. H. Sargent, *Table of Periodic Properties of the Elements*, H. B. Selby and Co., Melbourne, **1964**.
- [43] a) A. Bayler, A. Schier, G. A. Bowmaker, H. Schmidbaur, *J. Am. Chem. Soc.* **1996**, *118*, 7007; b) M.-S. Liao, W. H. E. Schwarz, *Acta Crystallogr. Sect. B* **1994**, *50*, 9; c) U. M. Tripathi, A. Bayler, H. Schmidbaur, *J. Chem. Soc. Dalton Trans.* **1997**, 2865.

Received: January 7, 1999 [F 1528]